Exponentially Stabilizing and Time-Varying Virtual Constraint Controllers for Dynamic Quadrupedal Bounding*

Joseph B. Martin V, Vinay R. Kamidi, Abhishek Pandala, Randall T. Fawcett, and Kaveh Akbari Hamed

***Abstract*— This paper aims to develop time-varying virtual constraint controllers that allow stable and agile bounding gaits for full-order hybrid dynamical models of quadrupedal locomotion. As opposed to state-based nonlinear controllers, time-varying controllers can initiate locomotion from zero velocity. Motivated by this property, we investigate the stability guarantees that can be provided by the time-varying approach. In particular, we systematically establish necessary and sufficient conditions that guarantee exponential stability of periodic orbits for time-varying hybrid dynamical systems utilizing the Poincaré return map. Leveraging the results of the presented proof, we develop time-varying virtual constraint controllers to stabilize bounding gaits of a 14 degree of freedom planar quadrupedal robot, Minitaur. A framework for choosing the parameters of virtual constraint controllers to achieve exponential stability is shown, and the feasibility of the analytical results is numerically validated in full-order simulation models of Minitaur.**

I. INTRODUCTION

Recent advances in control synthesis for dynamic, quadrupedal locomotion have shown great potential and close similarities to their biological counterparts, but controller synthesis approaches that address agile gaits for full-order dynamical models of quadrupeds are still developing. Our motivation is to design nonlinear controllers that can stabilize highly agile and dynamic motions with a particular focus on bounding gaits. By exploiting the potential of time-varying virtual constraints, we arrive at an exponentially stabilizing nonlinear controller for quadrupedal bounding. The choice of time as a gait phasing variable provides advantages such as allowing the system to start from zero velocity. We extend the Poincaré sections analysis to study the exponential stability properties of periodic gaits for hybrid dynamical models of legged locomotion with periodic and time-varying nonlinear controllers. We then demonstrate the effect of the parameters of the virtual constraint controllers on exponential stability and present an informed approach to guide the selection of outputs. The strength of the analytical results is finally demonstrated by numerical simulations of the full-order hybrid model for a quadrupedal test-bed.

*The work of V. R. Kamidi and A. Pandala is supported by the National Science Foundation (NSF) under the grant 1854898. The work of R. T. Fawcett is supported by the NSF under the grant 1906727. The work of K. Akbari Hamed is supported by the NSF under Grant Numbers 1923216. The content is solely the responsibility of the authors and does not necessarily represent the official views of the NSF.

J. Martin, V. R. Kamidi, A. Pandala, R. T. Fawcett, and K. Akbari Hamed are with the Department of Mechanical Engineering, Virginia Tech, Blacksburg, VA 24061, USA, {josephbmartinv, vinay28, agp19, randallf, kavehakbarihamed} @vt.edu

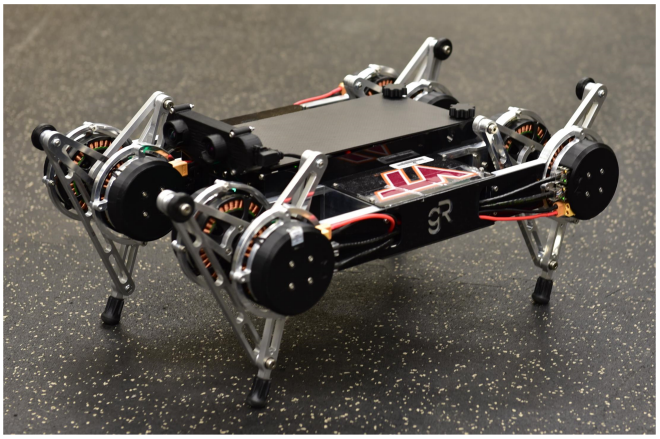

Fig. 1. Planar quadrupedal robot, Minitaur, designed by Ghost Robotics [1]. A full-order hybrid dynamical model is considered for the development of the controllers as well as the numerical studies.

A. Related Work and Motivation

The control of robotic legged locomotion was first formalized by the zero moment point (ZMP) control strategy, which stabilizes locomotion by driving the defined ZMP to remain within the support polygon made by the contact feet [2]. While this strategy has seen success on both bipedal [3]–[5] and quadrupedal [6] platforms, this method of control requires full actuation unlike the inherently underactuated locomotion of biological gaits. More recently, model predictive control (MPC) strategies which serve to predict the optimal sequence of control inputs to a finite time horizon have been used to control more robust and dynamic gait patterns, but are limited by the constraints of online computation, see e.g., [7]–[12]. Of the increasing variety of approaches that have become available to model locomotion problems, one such method gaining popularity in the legged locomotion community is that of the hybrid systems approach, see e.g., [13]–[23]. By casting the problem into continuous and discrete domains, it becomes possible to capture the evolution of the system over time through Lagrangian dynamics and to encode different physical and unilateral constraints that arise due to impacts. The hybrid nature of locomotion models has been addressed by a multitude of cutting-edge control approaches such as hybrid zero dynamics (HZD) [24], [25], transverse linearization [20], [26], hybrid reduction [27], [28], and controlled symmetries [19]. Of these methods, HZD and transverse linearization broadly address underactuation. HZD is an extension of zero dynamics to hybrid models of legged locomotion. In this approach, the coordination of the links is based on the description of output

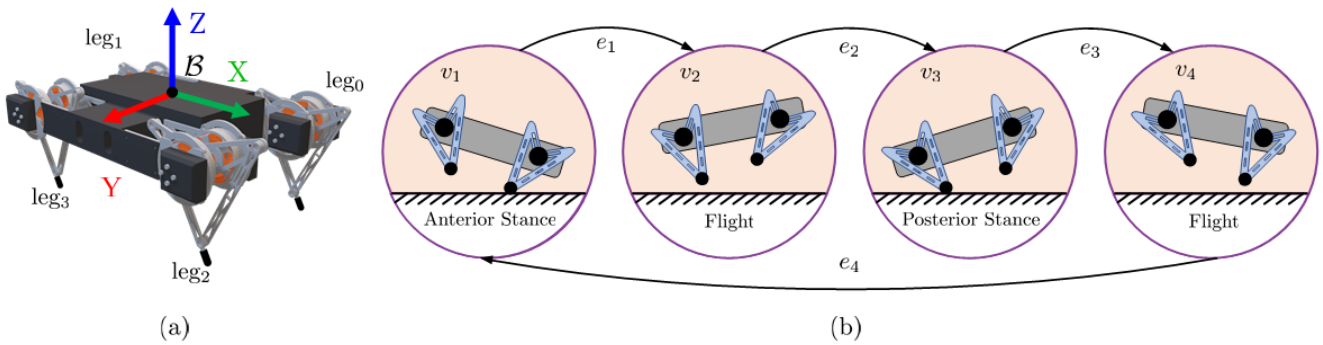

Fig. 2. An overview of Minitaur and the hybrid model of the bounding gait. (a) The floating base $\mathcal{B}$ and leg numbering convention for Minitaur. (b) Illustration of the directed cycle $\mathcal{G} = (\mathcal{V}, \mathcal{E})$ to represent the bounding gait with 4 continuous-time domains.

functions, known as virtual constraints, which are imposed via the action of a feedback controller (e.g., input-output (I-O) linearization). Virtual constraint controllers have been successfully implemented in simulation and practice on a wide variety of 2D and 3D bipedal robots [14], [15], [17], [29]–[32], lower-extremity prosthesis [33], [34], reduced-order models of quadrupedal locomotion [35], and full-order models of trotting, ambling, and walking gaits [36], [37]. Below, we summarize the advantages and disadvantages of two primary choices of the gait phasing parameter (i.e., state-based or time-based) utilized by HZD controllers to generate periodic orbits.

State-based parameterization is the widely used technique for HZD motion planning and control that considers a combination of state variables to define a strictly monotonic quantity, referred to as the phasing variable, to represent the progress of the robot on the gait. While asymptotic tracking and exponential stability of the gait are theoretically assured by state-based HZD controllers, they are frequently criticized for their reliance on highly accurate models and precise sensor measurements [38], [39]. In practice, the state-based controllers fail to account for sensor aggravations induced by impacts. This is further amplified for dynamic gaits such as bounding due to large impulse effects. Additionally, the method requires perturbation of the robot to induce velocity in the vicinity of the gait's domain of attraction, which may be practically infeasible for dynamic gaits. Alternatively, periodic orbits can be generated by choosing the time-varying parameterization [38], [39]. The key advantage of this approach is allowing the system to start from zero initial velocity, so long as the initial state is within the domain of attraction of the limit cycle. However, development of time-varying feedback controllers necessitates the use of the Poincaré sections analysis to validate orbital and exponential stability [40], [41].

The lack of a closed form solution for the Poincaré return map adds further difficulty to the construction of exponentially stabilizing HZD controllers for agile and dynamic gaits such as running and bounding. This observation has led to the use of event-based controllers, see e.g., [25], [35], [42], [43]. In this approach, a multi-level control strategy is adopted to execute the event-based controllers, wherein the low-level HZD controllers are implemented with adjustable parameters which are kept constant within the continuous-time domains and are then modified by the higher-level event-based controllers during the discrete transitions (i.e., in an event-based manner) such that all eigenvalues of the Jacobian linearizeation of the Poincaré return map becomes a Hurwitz matrix. One drawback of utilizing event-based controllers for addressing exponential stability of agile maneuvers is the potentially large delay between the occurrence of a disturbance and the event-based control effort.

In this paper, we aim to answer the following fundamental questions: 1) How can we design time-varying and exponentially stabilizing HZD controllers for bounding gaits without event-based actions? and 2) How can we choose the parameters of time-varying virtual constraints for stable bounding gaits?

B. Objectives and Contributions

We aim to systematically address the synthesis of a *single-level* exponentially stabilizing and time-varying HZD controller for highly dynamic bounding gaits without any higher-level event-based controllers. In what follows, we enumerate out significant contributions: 1) The paper presents necessary and sufficient conditions to analyze exponential stability of periodic orbits for hybrid dynamical systems with time-varying nonlinear controllers through the Poincaré sections analysis. 2) The paper addresses the development of time-varying HZD controllers to achieve stable bounding gaits for full-order hybrid models of quadrupedal locomotion. It studies the effects of the virtual constraints choice on stability and presents an approach to guide the output selections. 3) Analytical results of the paper are numerically verified on a full-order simulation model of a bounding gait for a quadrupedal platform, Minitaur (see Fig. 1), with 14 degrees of freedom (DOFs).

II. Hybrid Models of Locomotion

A. Robot Model

Minitaur is a 7.18kg quadrupedal robot developed by Ghost Robotics. Each leg, by design, is sagittaly constrained with two motors affixed to the ends of a four-bar linkage, resulting in 8 internal DOFs, that are encoded in the vector

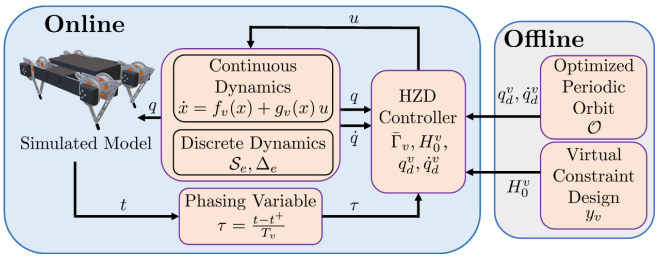

Fig. 3. Illustration of the single-level feedback control algorithm based on time-varying HZD control. The value t^+ represents the value of t at the end of the previous domain so the initial value of τ is zero.

q_m. Each motor pair in q_m is further parameterized by q_{i1} and q_{i2} for all $i \in \{0, 1, 2, 3\}$, where i denotes the leg number. Additionally, a base frame $\mathcal{B}$ is attached to the geometric center of the robot (see Fig. 2 (a)). The position and orientation of the frame $\mathcal{B}$ with respect to an inertial world frame is then represented by $q_b := \text{col}(q_x, q_y, q_z, q_{\text{roll}}, q_{\text{pitch}}, q_{\text{yaw}})$, in which $\text{col}(q_x, q_y, q_z)$ and $\text{col}(q_{\text{roll}}, q_{\text{pitch}}, q_{\text{yaw}})$ denote the Cartesian coordinates and absolute orientation of the robot, respectively. In our notation, "col" represents the column vector.

Four-bar legs are affixed to each of the motor pairs at the four corners of the base frame, consisting of two shorter upper bars and two longer lower bars which extend to the respective foot. Each motor in the pair rotates a respective upper bar, while the motion of the lower bars are determined from the closed kinematic chain. As the closed kinematic chain of the four-bar linkage leg structure produces modeling complexities, similar to [44], we use a coordinate transformation which maps the states of the motor pairs q_{i1} and q_{i2} to respective hip and knee coordinates of an equivalent two-bar structure for leg $i \in \{0, 1, 2, 3\}$. For each two-bar leg, the bars closest to the base frame are removed and rotation actuators are placed at the original motor location (the "hip") and the intersection of the remaining two links (the "knee"). After performing the linear transformations $q_{\text{H}i} := \frac{1}{2}(q_{i1} + q_{i2})$ and $q_{\text{K}i} := \frac{1}{2}(q_{i1} - q_{i2})$, where the subscripts "H" and "K" denote the hip and knee joints, respectively, we can introduce the generalized coordinates vector as follows:

$$q := \text{col}\{q_b, q_{\text{H}i}, q_{\text{K}i} \,|\, i = 0, 1, 2, 3\} \in \mathcal{Q} \tag{1}$$

for some configuration space $\mathcal{Q} \subset \mathbb{R}^{14}$. The state vector of the robot is taken as $x := \text{col}(q, \dot{q}) \in \text{T}\mathcal{Q} := \mathcal{Q} \times \mathbb{R}^{14}$.

B. Hybrid Dynamical Model of Locomotion

The hybrid model of locomotion is described by the following tuple as [36], [37]

$$\Sigma := (\mathcal{G}, \mathcal{X}, \mathcal{U}, \mathcal{D}, \mathcal{S}, \Delta, \mathcal{FG}), \tag{2}$$

where $\mathcal{G} = (\mathcal{V}, \mathcal{E})$ represents the directed graph of the locomotion pattern with the vertex set $\mathcal{V}$ denoting the continuous-time domains and the edge set $\mathcal{E} \subset \mathcal{V} \times \mathcal{V}$ representing the discrete-time transitions between continuous-time domains. The state manifolds and set of admissible controls are represented by $\mathcal{X} := \{\mathcal{X}_v\}_{v \in \mathcal{V}}$ and $\mathcal{U} := \{\mathcal{U}_v\}_{v \in \mathcal{V}}$, respectively, with $\mathcal{X}_v \subset \mathbb{R}^n$ and $\mathcal{U}_v \subset \mathbb{R}^m$, where $n = 28$ and $m = 8$. Moreover, $\mathcal{D} := \{\mathcal{D}_v\}_{v \in \mathcal{V}}$ with $\mathcal{D}_v \subset \mathcal{X}_v \times \mathcal{U}_v$ denotes the domains of admissibility on which 1) the ground reaction forces are feasible and 2) the unilateral constraints are satisfied. The evolution of the mechanical system during the continuous-time domain $v \in \mathcal{V}$ can be described by the input-affine state equation $\dot{x} = f_v(x) + g_v(x)\,u$. In particular, the equations of motion for the domain v can be expressed as follows:

$$\begin{aligned} D(q)\,\ddot{q} + H(q, \dot{q}) &= B\,u + J_v^\top(q)\,\lambda_v \\ J_v(q)\,\ddot{q} + \dot{J}_v(q, \dot{q})\,\dot{q} &= 0, \end{aligned} \tag{3}$$

where $D(q) \in \mathbb{R}^{14 \times 14}$ is the mass-inertia matrix, $H(q, \dot{q}) \in \mathbb{R}^{14}$ represents the Coriolis, centrifugal, and gravitational terms, and B is the input distribution matrix with the property rank $B = 8$. In addition, λ_v and $J_v(q)$ represent the Lagrange multipliers (i.e., ground reaction forces) and Jacobian matrix of the corresponding holonomic constraints, respectively. The set of guards in (2), i.e., $\mathcal{S} := \{\mathcal{S}_e\}_{e \in \mathcal{E}}$, then defines the set of states and controls $(x, u) \in \mathcal{D}$ on which the state trajectories encounter a discrete transition for the edge $e = (v \to v + 1)$. Furthermore, the set of discrete-time dynamics can be given by $\Delta := \{\Delta_e\}_{e \in \mathcal{E}}$, where upon intersection with $\mathcal{S}_e$ the state vector x evolves according to the discrete dynamics $x^+ = \Delta_e(x^-)$ [45]. The set of continuous-time dynamics is finally denoted by the set $\mathcal{FG} := \{(f_v, g_v)\}_{v \in \mathcal{V}}$.

In this paper, the hybrid model of a bounding gait is represented by a four-domain directed cycle of alternating stance and flight phases. Figure 2(b) illustrates the corresponding graph $\mathcal{G}$ with two stance and two flight phases.

***Remark** 1:* Since Minitaur is a planar robot, we are interested in studying the bounding gaits in the sagittal dynamics. For this purpose, we need to consider the Lagrangian dynamics (3) subject to some additional holonomic constraints arising from the confinement of the motion in the frontal and transversal planes. These conditions are expressed as $\ddot{q}_y = \ddot{q}_{\text{roll}} = \ddot{q}_{\text{yaw}} = 0$ and can be augmented to the Jacobian matrix $J_v(q)$ for all domains.

III. Exponential Stability Analysis of Periodic Gaits Under Time-Varying Controllers

The objective of this section is to investigate the exponential stability of dynamic gaits under time-varying and periodic feedback laws via the Poincaré sections analysis. This mathematical tool will help us to validate the convergence of state trajectories to a stable limit cycle and/or to synthesize real-time controllers that induce exponentially stable periodic solutions.

We will consider robot gaits as periodic solutions of the hybrid system Σ in (2). We investigate time-varying feedback controllers as follows:

$$u = \Gamma_v(\tau, x) \tag{4}$$

during the continuous-time domain $v \in \mathcal{V}$. Here, τ denotes the gait timing (i.e., phasing) variable which represents the progress of the robot on the gait. In particular, it is taken

as zero at the beginning of each domain (i.e., $\tau^+ = 0$) and evolves according to

$$\dot{\tau} = \frac{1}{T_v}, \tag{5}$$

where T_v is the desired elapsed time for the domain v. In (4), Γ_v is a continuously differentiable (i.e., $\mathcal{C}^1$) state law in terms of (τ, x). We assume that by employing the feedback controller (4), there is a periodic orbit for the closed-loop hybrid system. In particular, $\mathcal{O} := \{x = \varphi^*(t) \,|\, 0 \leq t < T\}$ denotes a periodic orbit for Σ, for some fundamental period $T > 0$ and some periodic solution $\varphi^*(t)$ with the property $\varphi^*(t+T) = \varphi^*(t)$ for all $t \geq 0$. According to the construction procedure, the state feedback law (4) is assumed to be periodic in τ with the period taken as 1, that is,

$$\Gamma_v(\tau + 1, x) = \Gamma_v(\tau, x) \tag{6}$$

for all $\tau \geq 0$, $x \in \mathcal{X}$, and $v \in \mathcal{V}$. In what follows, we study the dynamic stability of the periodic orbit $\mathcal{O}$ for the closed-loop hybrid system. For future purposes, we assume that $\mathcal{O}_v$ denotes the projection of $\mathcal{O}$ onto the state manifold of the domain v.

The evolution of the closed loop system during the domain $v \in \mathcal{V}$ can be described by the time-varying and periodic ordinary differential equation (ODE) $\dot{x} = f_v^{\text{cl}}(\tau, x) := f_v(x) + g_v(x)\,\Gamma_v(\tau, x)$. Let $\varphi_v(t, x_0)$ represent the state solution of $\dot{x} = f_v^{\text{cl}}(\tau, x)$ with the initial condition x_0 for all $t \geq 0$ in the maximal interval of existence. From [25, Theorem 4.3], one can present an equivalent single-domain hybrid model for the closed-loop hybrid system as follows:

$$\Sigma^{\text{cl}} : \begin{cases} \begin{bmatrix} \dot{x} \\ \dot{\tau} \end{bmatrix} = \begin{bmatrix} f_v^{\text{cl}}(\tau, x) \\ \frac{1}{T_v} \end{bmatrix}, & x^- \notin \mathcal{S}_e \\ \begin{bmatrix} x^+ \\ \tau^+ \end{bmatrix} = \begin{bmatrix} \Delta_e^{\text{cl}}(x^-) \\ 0 \end{bmatrix}, & x^- \in \mathcal{S}_e, \end{cases} \tag{7}$$

where $e = (v \to v+1)$ is the discrete transition after the domain v. Furthermore, Δ_e^{cl} represents the equivalent discrete-time dynamics that are composed of the flows of the remaining continuous-time domains as well as the discrete-time transitions. We note that since τ resets at the beginning of each domain, $\Delta_e^{\text{cl}}(x)$ does not depend on τ. In order to maintain compact notation, we define the augmented state variables as $x_a := \text{col}(x, \tau) \in \mathcal{X}_a := \mathcal{X} \times \mathbb{R}^+$. Using this notation, the augmented hybrid system can be represented by

$$\Sigma^{\text{cl}} : \begin{cases} \dot{x}_a = f_a^{\text{cl}}(x_a), & x_a^- \notin \mathcal{S}_a \\ x_a^+ = \Delta_a^{\text{cl}}(x_a^-), & x_a^- \in \mathcal{S}_a, \end{cases} \tag{8}$$

where $f_a^{\text{cl}}(x_a) := \text{col}(f_v^{\text{cl}}(\tau, x), \frac{1}{T_v})$, $\Delta_a^{\text{cl}}(x_a) := \text{col}(\Delta_e^{\text{cl}}(x), 0)$, and $\mathcal{S}_a := \mathcal{S}_e \times \mathbb{R}^+$ represent the augmented closed-loop vector field, augmented discrete-time transition, and augmented switching surface, respectively. We are now in a position to define the Poincaré map for the augmented system as $P_a : \mathcal{S}_a \to \mathcal{S}_a$ by

$$P_a(x_a) := \varphi_a\left(T_I\left(\Delta_a^{\text{cl}}(x_a)\right), \Delta_a^{\text{cl}}(x_a)\right), \tag{9}$$

where φ_a is the flow of the augmented ODE and $T_I(x_a(0))$ is the time elapsed for the augmented state solution to intersect $\mathcal{S}_a$. As per the above construction, there is a fixed point corresponding to the periodic orbit of the augmented system, that is,

$$P_a(x_a^*) = x_a^*, \tag{10}$$

where $x_a^* = \text{col}(x^*, 1)$, and x^* is the intersection of the closure of the periodic orbit with the switching surface, i.e., $\{x^*\} := \bar{\mathcal{O}} \cap \mathcal{S}_e$. The local exponential stability of the periodic orbit for the augmented system is equivalent to having all the eigenvalues of the Jacobian matrix of the Poincaré map inside the complex unit circle, i.e.,

$$\left|\text{eig}\left\{\frac{\partial P_a}{\partial x_a}(x_a^*)\right\}\right| < 1. \tag{11}$$

The augmented Poincaré map defined in (9) can be considered as an $n+1$-dimensional discrete-time system. The following theorem reduces the exponential stability problem of time-varying systems into that of an n-dimensional system.

***Theorem** 1: **(Poincaré Analysis for Periodic Orbits of Time-Varying Hybrid Systems):** Consider the time-varying state feedback laws* (4)*, in which the time-based phasing variable evolves according to* (5) *and resets on the switching manifolds as $\tau^+ = 0$. Then, the following statements hold.*

1) *The Jacobian linearization of the Poincaré map for the augmented system takes the following structure*

$$\frac{\partial P_a}{\partial x_a}(x_a^*) = \begin{bmatrix} \frac{\partial P_x}{\partial x}(x^*, 1) & 0 \\ \frac{\partial P_\tau}{\partial x}(x^*, 1) & 0 \end{bmatrix}, \tag{12}$$

   where $P_a = col(P_x, P_\tau)$ is a decomposition corresponding to (x, τ), i.e., $P_x \in \mathbb{R}^n$ and $P_\tau \in \mathbb{R}$.

2) *The periodic orbit $\mathcal{O}$ is orbitally exponentially stable for the closed-loop hybrid system, if, and only if,*

$$\left|eig\left\{\frac{\partial P_x}{\partial x}(x^*, 1)\right\}\right| < 1. \tag{13}$$

Proof: From [46, Theorem D.1] and chain rule, the Jacobian linearization of the Poincaré map can be expressed in a closed-form solution as follows:

$$\frac{\partial P_a}{\partial x_a}(x_a^*) = \underbrace{\left(I_{n+1} - \frac{f_a^{\text{cl}}(x_a^*)\frac{\partial s_a}{\partial x_a}(x_a^*)}{\frac{\partial s_a}{\partial x_a}(x_a^*) f_a^{\text{cl}}(x_a^*)}\right)}_{:=\Pi(x_a^*)} \Phi_a(T_v) \frac{\partial \Delta_a^{\text{cl}}}{\partial x_a}(x_a^*), \tag{14}$$

where I_{n+1} is the identity matrix of dimension $n+1$, $\Pi(x_a^*)$ is referred to as the saltation matrix, and

$$\Phi_a(t) := \frac{\partial \varphi_a}{\partial x_0}(t, x_0) \in \mathbb{R}^{(n+1)\times(n+1)} \tag{15}$$

represents the trajectory sensitivity matrix. In addition, the augmented switching surface $\mathcal{S}_a = \mathcal{S}_e \times \mathbb{R}^+$ can be considered as a zero-level set of a differential function $s_a(x_a)$ that only depends on x, that is, $s_a(x_a) = s_a(x)$. As $f_a^{\text{cl}}(x_a^*) = \text{col}(f_v^{\text{cl}}(x_a^*), \frac{1}{T_v})$ and $\frac{\partial s_a}{\partial x_a}(x_a^*) = [\frac{\partial s_a}{\partial x}(x_a^*)\ 0]$, one can simplify the saltation matrix $\Pi(x_a^*)$ as follows:

$$\Pi(x_a^*) = \begin{bmatrix} I_n & 0 \\ 0 & 1 \end{bmatrix} - \frac{1}{\frac{\partial s_a}{\partial x}(x_a^*) f_a^{\text{cl}}(x_a^*)} \begin{bmatrix} f_v^{\text{cl}}(x_a^*)\frac{\partial s_a}{\partial x}(x_a^*) & 0 \\ \frac{\partial s_a}{\partial x}(x_a^*)\frac{1}{T_v} & 0 \end{bmatrix} \tag{16}$$

which can be decomposed into (x, τ) coordinates as

$$\Pi(x_a^*) = \begin{bmatrix} \Pi_{xx} & 0 \\ \Pi_{\tau x} & 1 \end{bmatrix} \tag{17}$$

From the variational equation [46, Appendix B], the state trajectory sensitivity matrix satisfies the following matrix differential equation

$$\begin{aligned} \dot{\Phi}_a(t) &= A_a(t)\,\Phi_a(t) \\ \Phi_a(0) &= I_{n+1} \\ A_a(t) &:= \frac{\partial f_a^{\text{cl}}}{\partial x_a}(\varphi_a^*(t)), \end{aligned} \tag{18}$$

in which $\varphi_a^*(t)$ denotes the augmented periodic trajectory. The trajectory sensitivity matrix as well as the Jacobian linearization of the augmented vector field along the periodic trajectory can be decomposed into (x, τ) coordinates as follows:

$$\begin{aligned} \Phi_a(t) &= \begin{bmatrix} \Phi_{xx}(t) & \Phi_{x\tau}(t) \\ \Phi_{\tau x}(t) & \Phi_{\tau\tau}(t) \end{bmatrix} \\ A_a(t) &= \begin{bmatrix} \frac{\partial f_v^{\text{cl}}}{\partial x}(\tau, x) & \frac{\partial f_v^{\text{cl}}}{\partial \tau}(\tau, x) \\ 0 & 0 \end{bmatrix} := \begin{bmatrix} A_{xx}(t) & A_{x\tau}(t) \\ 0 & 0 \end{bmatrix}. \end{aligned} \tag{19}$$

Equation (19) reduces the variational equation into the following matrix differential equations

$$\dot{\Phi}_{xx}(t) = A_{xx}(t)\,\Phi_{xx}(t), \qquad \Phi_{xx}(0) = I_n \tag{20}$$

$$\dot{\Phi}_{x\tau}(t) = A_{xx}(t)\,\Phi_{x\tau}(t) + A_{x\tau}(t), \quad \Phi_{x\tau}(0) = 0 \tag{21}$$

$$\Phi_{\tau x}(t) \equiv 0, \tag{22}$$

$$\Phi_{\tau\tau}(t) \equiv 1. \tag{23}$$

Combining (17) and (20)-(23), we can simplify the Jacobian linearization of the Poincaré map as follows:

$$\begin{aligned} \frac{\partial P_a}{\partial x_a}(x_a^*) &= \begin{bmatrix} \Pi_{xx} & 0 \\ \Pi_{\tau x} & 1 \end{bmatrix} \begin{bmatrix} \Phi_{xx}(T_v) & \Phi_{x\tau}(T_v) \\ 0 & 1 \end{bmatrix} \underbrace{\begin{bmatrix} D_{xx} & 0 \\ 0 & 0 \end{bmatrix}}_{\frac{\partial \Delta_a^{\text{cl}}}{\partial x_a}(x_a^*)} \\ &= \begin{bmatrix} \Pi_{xx}\,\Phi_{xx}(T_v)\,D_{xx} & 0 \\ \Pi_{\tau x}\,\Phi_{xx}(T_v)\,D_{xx} & 0 \end{bmatrix}, \end{aligned} \tag{24}$$

in which $D_{xx} := \frac{\partial \Delta_e^{\text{cl}}}{\partial x}(x^*)$. This completes the proof of Part (1). With the above structure of the Jacobian matrix, the eigenvalues become

$$\begin{aligned} \text{eig}\left\{\frac{\partial P_a}{\partial x_a}(x_a^*)\right\} &= \text{eig}\left\{\Pi_{xx}\,\Phi_{xx}(T_v)\,D_{xx}\right\} \cup \{0\} \\ &= \text{eig}\left\{\frac{\partial P_x}{\partial x}(x_a^*)\right\} \cup \{0\} \end{aligned} \tag{25}$$

which completes the proof of Part (2). ■

IV. Design of Parameterized and Time-Varying Virtual Constraints for Bounding Gaits

The objective of this section is to present virtual constraint controllers that allow exponentially stable agile and dynamic bounding gaits. Virtual constraints are kinematic constraints that are defined to coordinate the motion of links. We consider a set of parameterized virtual constraint controllers and will then utilize Theorem 1 to study the effect of parameters on the stability of bounding gaits. We will also present a guide on how to choose the stabilizing parameters.

In this paper, the virtual constraints are defined as follows:

$$y_v(\tau, x) := H_0^v(q - q_v^d(\tau)), \tag{26}$$

where H_0^v is an output matrix to be determined and $q_v^d(\tau)$ represents the desired evolution of the configuration variables during the continuous-time domain v. For later purposes, $h_0^v(q) := H_0^v\, q$ is referred to as the controlled variables. Our previous work in HZD [23], [47] has shown that the proper selection of the controlled variables $h_0^v(q)$ directly affects the stability of dynamic gaits.

To choose the controlled variables or equivalently the output matrices, we first start with controlling the internal and actuated DOFs of the robot. Section V will show that this cannot stabilize the bounding gait. To stabilize the gait, we then modify the controlled variables by adding terms that correspond to the pitch angle q_{pitch}. This will let the HZD controller take into account the deviation from the desired pitch angles in the stance and flight phases. It will also allow the robot to land at proper angles at the end of flight phases to recover from instability. This procedure is mathematically done by adding the pitch angle to the internal controlled variables via some weighting factors α_v and β_v that will be tuned in Section V through Theorem 1. Additionally, the dimension of the virtual constraints for stance phases is reduced from $\mathbb{R}^m$ to $\mathbb{R}^{m-2}$ due to the closed kinematic chain formed by the two front or the two rear stance legs, therefore the outputs associated with the stance hips and knees respectively are averaged. To make this notion more precise, the controlled variables for the first stance and flight phases are chosen as follows:

$$H_0^1 q := \begin{bmatrix} \frac{1}{2}q_{\text{H0}} + \frac{1}{2}q_{\text{H2}} + \alpha_1 q_{\text{pitch}} \\ q_{\text{H1}} \\ q_{\text{H3}} \\ \frac{1}{2}q_{\text{K0}} + \frac{1}{2}q_{\text{K2}} + \beta_1 q_{\text{pitch}} \\ q_{\text{K1}} \\ q_{\text{K3}} \end{bmatrix}, \tag{27}$$

$$H_0^2 q := \begin{bmatrix} q_{\text{H0}} + \alpha_2 q_{\text{pitch}} \\ q_{\text{H2}} + \alpha_2 q_{\text{pitch}} \\ q_{\text{H1}} \\ q_{\text{H3}} \\ q_{\text{K0}} + \beta_2 q_{\text{pitch}} \\ q_{\text{K2}} + \beta_2 q_{\text{pitch}} \\ q_{\text{K1}} \\ q_{\text{K3}} \end{bmatrix}. \tag{28}$$

In (27), we control the average knee and hip angles for the front stance legs, while allowing feedback from the pitch angle via the coefficients α_1 and β_1 respectively. The angles of the rear legs (i.e., swing legs) are controlled individually and without influence from the pitch angle. Equation (28) addresses the controlled variables for the flight phase. Here, each hip angle of the rear legs–which will land at the end

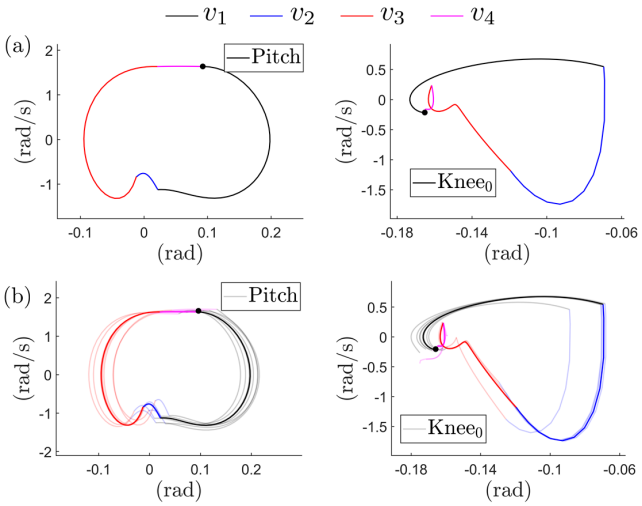

Fig. 4. (a) Limit cycles of q_{pitch} and q_{K0} for the periodic bounding gait. (b) Phase portraits for the motions of q_{pitch} and q_{K0} over 20 cycles starting from a perturbed initial condition. Convergence to the limit cycle is clear.

of the phase–experiences identical pitch feedback via α_2, and the rear knee angles are controlled in the same manner with respect to β_2. The controlled variables of the front legs are uninfluenced by the pitch angle. Similar parametrization can be presented for domains 3 and 4 with different α and β values. Differentiating the holonomic outputs along the continuous-time dynamics of domain v results in the following output dynamics

$$\begin{aligned} \ddot{y}_v &= \mathcal{L}_{g_v}\mathcal{L}_{f_v} y_v(\tau, x)\, u + \mathcal{L}_{f_v}^2 y_v(\tau, x) \\ &= -K_p\, y_v - K_d\, \dot{y}_v \end{aligned} \tag{29}$$

in which "$\mathcal{L}$" denotes the Lie derivative, and K_p and K_d are positive definite matrices and hence, the origin is exponentially stable for (29). From the output dynamics, one can solve for the minimum 2-norm (i.e., minimum power) I-O linearizing controller as follows:

$$\begin{aligned} u &= \Gamma_v\,(\tau, x) \\ &:= -\,(\mathcal{L}_{g_v}\mathcal{L}_{f_v} y_v)^{\dagger}(\mathcal{L}_{f_v}^2 y_v + K_p\, y_v + K_d\, \dot{y}_v), \end{aligned} \tag{30}$$

where the superscript "†" represents the pseudoinverse operator as the decoupling matrix $\mathcal{L}_{g_v}\mathcal{L}_{f_v} y_v$ is 6×8 during the stance phases.

V. Numerical Simulations

This section provides details of numerical simulations which validate the performance of the proposed time-varying, single-level HZD controller on the full-order hybrid model of locomotion.

A. Direct Collocation-Based HZD Gait Planning

The complexity associated with generating a feasible periodic orbit $\mathcal{O}$ for the nonlinear and full-order hybrid model of a quadruped bounding gait is addressed with a direct collocation-based HZD gait planning method [48] which converts the path planning into a nonlinear programming (NLP) problem that can be effectively solved by IPOPT [49]. The resulting gait is ensured to satisfy position, velocity, and torque limits while taking into account the unilateral and friction cone conditions. A cost function $J = \int_0^T u^{\top}(t)\, R\, u(t)\, \mathrm{d}t$ is minimized to ensure the efficiency of the resulting gait. The NLP has 8208 decision variables, 3996 equality constraints, and 6684 inequality constraints and produces a feasible gait trajectory in 282.27 seconds on a 64-bit installation of Windows 10 with 16GB of RAM and an 8-core Intel i7-9800X 3.8GHz processor. The gait has an average speed of 0.36 (m/s). Figure 4 (a) depicts the corresponding limit cycles for two degrees of freedom of the robot. Color denotes different domains of the bounding gait.

B. Poincaré Sections Analysis

As a direct result of Theorem 1, the exponential stability of the periodic orbit $\mathcal{O}$ for the time-varying closed-loop hybrid system can be verified via the proposed Poincaré sections analysis. The Poincaré section is taken at $\tau = 1$ for the anterior stance phase. We remark that the results of Theorem 1 consider the Poincaré map as an $n+1$-dimensional map to simplify the presentation, but it is indeed an n-dimensional partial map from $\mathcal{S}_a$ back to $\mathcal{S}_a$. To take this point into account, one would need to remove a dependent coordinate from the state vector. Without loss of generality, we eliminate the q_z component which represents the height of the base frame $\mathcal{B}$. We also remark that as the robot travels in the x-direction, it lacks periodicity in the q_x component and thus, there will be an eigenvalue 1 for the Jacobian matrix $\frac{\partial P_x}{\partial x}(x_a^*)$. Consequently, to achieve exponential stability, all the remaining eigenvalues must lie inside the unit circle.

C. Tuning HZD Controllers and Closed-Loop Simulations

We now employ the parameterized virtual constraints controller to stabilize the bounding gait generated by the NLP. Without tuning (i.e., $\alpha_v{=}\beta_v{=}0$ for all $v \in \mathcal{V}$), the dominant eigenvalues and spectral radius of the Jacobian of the Poincaré map about the fixed point are $\{15.015, 1.0000, 0.0898 \pm 0.2418i\}$ and 15.015, respectively, and thus the gait is unstable. In order to achieve exponential stability, we employ our previously developed algorithm that is an iterative sequence of optimization problems including bilinear matrix inequalities (BMIs) [23], [47] to the results of Theorem 1. The BMI algorithm iteratively updates the HZD controller parameters $\{\alpha_v, \beta_v\}$ until all eigenvalues of the Jacobian matrix $\frac{\partial P_x}{\partial x}(x_a^*)$ are within the unit circle. The algorithm successfully converges to a set of stabilizing parameters $\{\alpha_v\}_{v\in\mathcal{V}} = \{0.8072,\ 2.7925,\ -0.9384,\ 1.1633\}$ and $\{\beta_v\}_{v\in\mathcal{V}} = \{-0.1027,\ -1.8087,\ -0.0005,\ 0.7405\}$ after a finite number of iterations for which the dominant eigenvalues of the Jacobian matrix become $\{1.0000,\ -0.0509 \pm 1.6145i,\ -0.0621\}$. As expected, the eigenvalue of 1 corresponds to the non-periodic evolution of q_x, while all of the remaining eigenvalues are well within the unit circle. Hence, the gait is exponentially stable. Figure 4 (b) depicts the phase portraits for the motion of q_{pitch} and q_{K0} initialized off of the limit cycle obtained from the direct collocation optimization. Figure 5 illustrates the time profile of the virtual constraints and torque inputs versus time. We remark

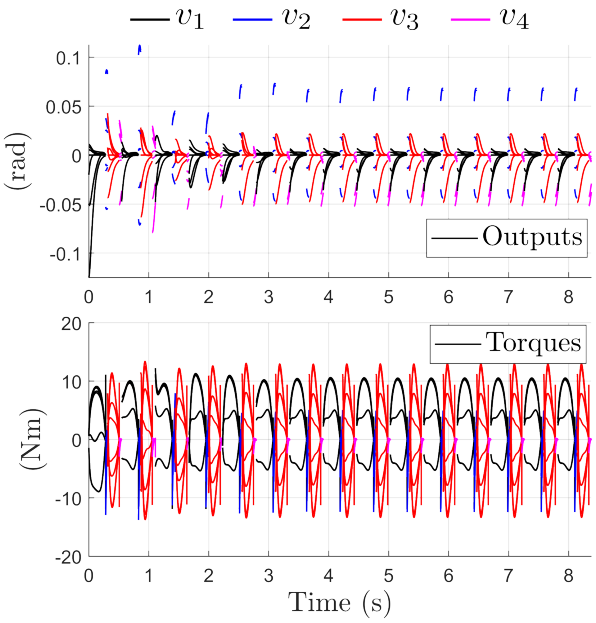

Fig. 5. Simulated outputs y_v and torques u over 15 cycles from a perturbed initial condition. Outputs are also shown converging to zero during each stance phase. The discontinuities in the plotted outputs arise due to the fact that only the active outputs as defined by H_v^0 are plotted for each domain v. The practical feasibility of the torques is displayed by the bounded operating range of approximately ± 10 Nm.

that the Minitaur platform makes use of direct-drive motors with no gear reduction system. Figure 6 finally displays snapshots of the simulated gait trajectory. Animations of these simulations can be found online.[1]

VI. Conclusions

This paper presented a methodology for the design and analysis of single-level and time-varying HZD controllers that exponentially stabilize agile and dynamic gaits for full-order hybrid dynamical models of quadrupedal locomotion. The Poincaré sections approach was extended to provide necessary and sufficient conditions that guarantee exponential stability of periodic gaits under time-varying nonlinear controllers. A set of parameterized virtual constraints is proposed to address agile bounding gaits. A formal approach is presented to tune the parameters of the virtual constraint controllers. To demonstrate the power of the approach, the analytical results were used to synthesize a stabilizing and time-varying HZD controller for a full-order hybrid model that describes bounding gaits of the quadrupedal robot Minitaur with 28 state variables and 8 control inputs.

For future work, we will investigate the design of robust-optimal time-varying HZD controllers that can address robust and agile quadrupedal locomotion over rough terrains. Additional simulations will address controller response to unexpected disturbances and modeling errors and gaits which a zero velocity initial condition within their respective domains of attraction. We will also experimentally validate the HZD-based bounding gait for the Minitaur platform.

[1]https://youtu.be/CosR7cd1eVo

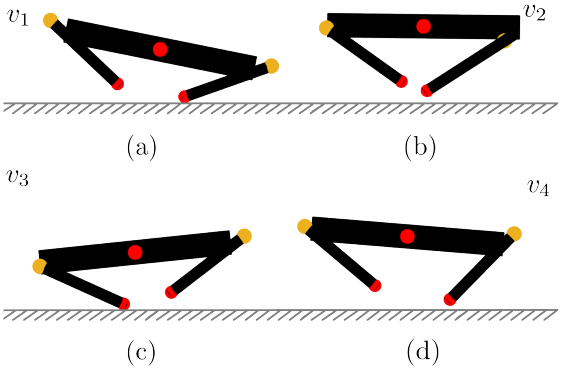

Fig. 6. Simulation snapshots illustrating the bounding sequence of Minitaur as a result of the proposed HZD controller. (a) Anterior Stance (b) First Flight Phase (c) Posterior Stance Phase (d) Second Flight Phase.

References

[1] Ghost Robotics, https://www.ghostrobotics.io/.

[2] M. Vukobratović, B. Borovac, and D. Surla, *Dynamics of Biped Locomotion*. Springer, 1990.

[3] K. Hirai, M. Hirose, Y. Haikawa, and T. Takenaka, "The development of Honda humanoid robot," in *Robotics and Automation. Proceedings IEEE International Conference on*, vol. 2, May 1998, pp. 1321–1326 vol.2.

[4] H.-O. Lim, Y. Yamamoto, and A. Takanishi, "Control to realize human-like walking of a biped humanoid robot," in *Systems, Man, and Cybernetics, IEEE International Conference on*, vol. 5, 2000, pp. 3271–3276 vol.5.

[5] J. Yamaguchi, E. Soga, S. Inoue, and A. Takanishi, "Development of a bipedal humanoid robot-control method of whole body cooperative dynamic biped walking," in *Robotics and Automation. Proceedings IEEE International Conference on*, vol. 1, 1999, pp. 368–374 vol.1.

[6] T. Akbas, S. Eskimez, S. Ozel, Adak, K. Fidan, and K. Erbatur, "Zero moment point based pace reference generation for quadruped robots via preview control," *International Workshop on Advanced Motion Control, AMC*, 03 2012.

[7] F. Borrelli, A. Bemporad, and M. M., *Predictive Control for Linear and Hybrid Systems*. Cambridge University Press, 2017.

[8] J. Di Carlo, P. M. Wensing, B. Katz, G. Bledt, and S. Kim, "Dynamic locomotion in the MIT Cheetah 3 through convex model-predictive control," in *2018 IEEE/RSJ International Conference on Intelligent Robots and Systems (IROS)*, Oct 2018, pp. 1–9.

[9] Y. Ding, A. Pandala, and H. Park, "Real-time model predictive control for versatile dynamic motions in quadrupedal robots," in *2019 International Conference on Robotics and Automation (ICRA)*, May 2019, pp. 8484–8490.

[10] O. Villarreal, V. Barasuol, P. Wensing, and C. Semini, "MPC-based controller with terrain insight for dynamic legged locomotion," *arXiv preprint arXiv:1909.13842*, 2019.

[11] M. Neunert, M. Stäuble, M. Giftthaler, C. D. Bellicoso, J. Carius, C. Gehring, M. Hutter, and J. Buchli, "Whole-body nonlinear model predictive control through contacts for quadrupeds," *IEEE Robotics and Automation Letters*, vol. 3, no. 3, pp. 1458–1465, July 2018.

[12] G. Bledt, P. M. Wensing, and S. Kim, "Policy-regularized model predictive control to stabilize diverse quadrupedal gaits for the mit cheetah," in *2017 IEEE/RSJ International Conference on Intelligent Robots and Systems (IROS)*, Sep. 2017, pp. 4102–4109.

[13] J. Grizzle, G. Abba, and F. Plestan, "Asymptotically stable walking for biped robots: Analysis via systems with impulse effects," *Automatic Control, IEEE Transactions on*, vol. 46, no. 1, pp. 51–64, Jan 2001.

[14] A. Ames, K. Galloway, K. Sreenath, and J. Grizzle, "Rapidly exponentially stabilizing control Lyapunov functions and hybrid zero dynamics," *Automatic Control, IEEE Transactions on*, vol. 59, no. 4, pp. 876–891, April 2014.

[15] K. Sreenath, H.-W. Park, I. Poulakakis, and J. W. Grizzle, "Compliant hybrid zero dynamics controller for achieving stable, efficient and fast bipedal walking on MABEL," *The International Journal of Robotics Research*, vol. 30, no. 9, pp. 1170–1193, Aug. 2011.

[16] H. Dai and R. Tedrake, "Optimizing robust limit cycles for legged locomotion on unknown terrain," in *Decision and Control, IEEE 51st Annual Conference on*, Dec 2012, pp. 1207–1213.

[17] C. O. Saglam and K. Byl, "Meshing hybrid zero dynamics for rough terrain walking," in *2015 IEEE International Conference on Robotics and Automation (ICRA)*, May 2015, pp. 5718–5725.

[18] A. M. Johnson, S. A. Burden, and D. E. Koditschek, "A hybrid systems model for simple manipulation and self-manipulation systems," *The International Journal of Robotics Research*, vol. 35, no. 11, pp. 1354–1392, 2016.

[19] M. Spong and F. Bullo, "Controlled symmetries and passive walking," *Automatic Control, IEEE Transactions on*, vol. 50, no. 7, pp. 1025–1031, July 2005.

[20] I. Manchester, U. Mettin, F. Iida, and R. Tedrake, "Stable dynamic walking over uneven terrain," *The International Journal of Robotics Research*, vol. 30, no. 3, pp. 265–279, 2011.

[21] R. Vasudevan, *Hybrid System Identification via Switched System Optimal Control for Bipedal Robotic Walking*. Cham: Springer International Publishing, 2017, pp. 635–650.

[22] K. Akbari Hamed and R. D. Gregg, "Decentralized event-based controllers for robust stabilization of hybrid periodic orbits: Application to underactuated 3d bipedal walking," *IEEE Transactions on Automatic Control*, pp. 1–16, July 2018.

[23] K. Akbari Hamed, B. Buss, and J. Grizzle, "Exponentially stabilizing continuous-time controllers for periodic orbits of hybrid systems: Application to bipedal locomotion with ground height variations," *The International Journal of Robotics Research*, vol. 35, no. 8, pp. 977–999, 2016.

[24] E. Westervelt, J. Grizzle, and D. Koditschek, "Hybrid zero dynamics of planar biped walkers," *Automatic Control, IEEE Transactions on*, vol. 48, no. 1, pp. 42–56, Jan 2003.

[25] E. Westervelt, J. Grizzle, C. Chevallereau, J. Choi, and B. Morris, *Feedback Control of Dynamic Bipedal Robot Locomotion*. Taylor & Francis/CRC, 2007.

[26] A. Shiriaev, L. Freidovich, and S. Gusev, "Transverse linearization for controlled mechanical systems with several passive degrees of freedom," *Automatic Control, IEEE Transactions on*, vol. 55, no. 4, pp. 893–906, April 2010.

[27] A. D. Ames, R. D. Gregg, E. D. B. Wendel, and S. Sastry, "On the geometric reduction of controlled three-dimensional bipedal robotic walkers," in *Lagrangian and Hamiltonian Methods for Nonlinear Control 2006*. Berlin, Heidelberg: Springer Berlin Heidelberg, 2007, pp. 183–196.

[28] R. D. Gregg and M. W. Spong, "Reduction-based control of three-dimensional bipedal walking robots," *The International Journal of Robotics Research*, vol. 29, no. 6, pp. 680–702, May 2010.

[29] C. Chevallereau, G. Abba, Y. Aoustin, F. Plestan, E. Westervelt, C. Canudas-de Wit, and J. Grizzle, "RABBIT: A testbed for advanced control theory," *Control Systems Magazine, IEEE*, vol. 23, no. 5, pp. 57–79, Oct 2003.

[30] A. Ramezani, J. Hurst, K. Akbai Hamed, and J. Grizzle, "Performance analysis and feedback control of ATRIAS, a three-dimensional bipedal robot," *Journal of Dynamic Systems, Measurement, and Control December, ASME*, vol. 136, no. 2, December 2013.

[31] A. Hereid, C. M. Hubicki, E. A. Cousineau, and A. D. Ames, "Dynamic humanoid locomotion: A scalable formulation for HZD gait optimization," *IEEE Transactions on Robotics*, pp. 1–18, 2018.

[32] A. E. Martin, D. C. Post, and J. P. Schmiedeler, "The effects of foot geometric properties on the gait of planar bipeds walking under HZD-based control," *The International Journal of Robotics Research*, vol. 33, no. 12, pp. 1530–1543, 2014.

[33] R. Gregg and J. Sensinger, "Towards biomimetic virtual constraint control of a powered prosthetic leg," *Control Systems Technology, IEEE Transactions on*, vol. 22, no. 1, pp. 246–254, Jan 2014.

[34] H. Zhao, J. Horn, J. Reher, V. Paredes, and A. D. Ames, "Multicontact locomotion on transfemoral prostheses via hybrid system models and optimization-based control," *IEEE Transactions on Automation Science and Engineering*, vol. 13, no. 2, pp. 502–513, 2016.

[35] Q. Cao and I. Poulakakis, "Quadrupedal running with a flexible torso: control and speed transitions with sums-of-squares verification," *Artificial Life and Robotics*, vol. 21, no. 4, pp. 384–392, Dec 2016.

[36] K. A. Hamed, W. Ma, and A. D. Ames, "Dynamically stable 3d quadrupedal walking with multi-domain hybrid system models and virtual constraint controllers," in *2019 American Control Conference (ACC)*, July 2019, pp. 4588–4595.

[37] W. Ma, K. A. Hamed, and A. D. Ames, "First steps towards full model based motion planning and control of quadrupeds: A hybrid zero dynamics approach," in *2019 IEEE/RSJ International Conference on Intelligent Robots and Systems (IROS)*, Nov 2019, pp. 5498–5503.

[38] S. Kolathaya, A. Hereid, and A. D. Ames, "Time dependent control Lyapunov functions and hybrid zero dynamics for stable robotic locomotion," in *2016 American Control Conference (ACC)*, July 2016, pp. 3916–3921.

[39] W. Ma, S. Kolathaya, E. R. Ambrose, C. M. Hubicki, and A. D. Ames, "Bipedal robotic running with DURUS-2D: Bridging the gap between theory and experiment," in *Proceedings of the 20th International Conference on Hybrid Systems: Computation and Control*. ACM, 2017, pp. 265–274.

[40] B. Morris and J. Grizzle, "Hybrid invariant manifolds in systems with impulse effects with application to periodic locomotion in bipedal robots," *Automatic Control, IEEE Transactions on*, vol. 54, no. 8, pp. 1751–1764, Aug 2009.

[41] S. Veer, Rakesh, and I. Poulakakis, "Input-to-state stability of periodic orbits of systems with impulse effects via poincaré analysis," *IEEE Transactions on Automatic Control*, vol. 64, no. 11, pp. 4583–4598, Nov 2019.

[42] K. Sreenath, H.-W. Park, I. Poulakakis, and J. Grizzle, "Embedding active force control within the compliant hybrid zero dynamics to achieve stable, fast running on MABEL," *The International Journal of Robotics Research*, vol. 32, no. 3, pp. 324–345, 2013.

[43] K. Akbari Hamed, N. Sadati, W. Gruver, and G. Dumont, "Exponential stabilisation of periodic orbits for running of a three-dimensional monopedal robot," *Control Theory Applications, IET*, vol. 5, no. 11, pp. 1304–1320, July 2011.

[44] J. Tan, T. Zhang, E. Coumans, A. Iscen, Y. Bai, D. Hafner, S. Bohez, and V. Vanhoucke, "Sim-to-real: Learning agile locomotion for quadruped robots," in *Robotics: Science and Systems (RSS)*, 2018.

[45] Y. Hurmuzlu and D. B. Marghitu, "Rigid body collisions of planar kinematic chains with multiple contact points," *The International Journal of Robotics Research*, vol. 13, no. 1, pp. 82–92, 1994.

[46] T. Parker and L. Chua, *Practical Numerical Algorithms for Chaotic Systems*. Springer, 1989.

[47] K. Akbari Hamed and R. D. Gregg, "Decentralized feedback controllers for robust stabilization of periodic orbits of hybrid systems: Application to bipedal walking," *Control Systems Technology, IEEE Transactions on*, vol. 25, no. 4, pp. 1153–1167, July 2017.

[48] A. Hereid and A. D. Ames, "Frost: Fast robot optimization and simulation toolkit," in *IEEE/RSJ International Conference on Intelligent Robots and Systems (IROS)*. Vancouver, BC, Canada: IEEE/RSJ, Sep. 2017.

[49] A. Wächter and L. T. Biegler, "On the implementation of an interior-point filter line-search algorithm for large-scale nonlinear programming," *Mathematical programming*, vol. 106, no. 1, pp. 25–57, 2006.